

## **Lidar Measurement of Rocket Exhaust Plume Dispersion and Layering in the Stratosphere**

**Phan D. Dao**  
**Anthony Dentamaro**

**16 Sep 1999**

**Approved for Public Release; Distribution Unlimited**



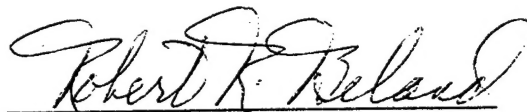
**AIR FORCE RESEARCH LABORATORY**  
**Space Vehicles Directorate**  
**29 Randolph Rd**  
**AIR FORCE MATERIEL COMMAND**  
**Hanscom AFB, MA 01731-3010**

---

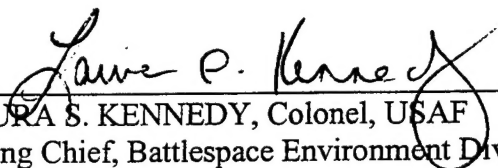
"This technical report has been reviewed and is approved for publication."



PHAN D. DAO  
Author



Robert R. Beland, Chief  
Tactical Environmental Support Branch



LAURA S. KENNEDY, Colonel, USAF  
Acting Chief, Battlespace Environment Division

This report has been reviewed by the ESC Public Affairs Office (PA) and is releasable to the National Technical Information Service (NTIS).

Qualified requestors may obtain additional copies from the Defense Technical Information Center (DTIC). All others should apply to the National Technical Information Service (NTIS).

If your address has changed, if you wish to be removed from the mailing list, or if the addressee is no longer employed by your organization, please notify PL/IM, 29 Randolph Road, Hanscom AFB, MA. 01731-3010. This will assist us in maintaining a current mailing list.

Do not return copies of this report unless contractual obligations or notices on a specific document require that it be returned.

REPORT DOCUMENTATION PAGE			Form Approved OMB No. 0704-0188	
Public reporting burden for this collection of information is estimated to average 1 hour per response, including the time for reviewing instructions, searching existing data sources, gathering and maintaining the data needed, and completing and reviewing the collection of information. Send comments regarding this burden estimate or any other aspect of this collection of information, including suggestions for reducing this burden, to Washington Headquarters Services, Directorate for Information Operations and Reports, 1215 Jefferson Davis Highway, Suite 1204, Arlington, VA 22202-4302, and to the Office of Management and Budget, Paperwork Reduction Project (0704-0188), Washington, DC 20503.				
1. AGENCY USE ONLY (Leave blank)		2. REPORT DATE 16 Sep 1999		3. REPORT TYPE AND DATES COVERED Scientific, Final
4. TITLE AND SUBTITLE Lidar Measurement of Rocket Exhaust Plume Dispersion and Layering in the Stratosphere			5. FUNDING NUMBERS PR CLPM TA BS WU 88	
6. AUTHOR(S) Phan D. Dao Anthony Dentamaro*				
7. PERFORMING ORGANIZATION NAME(S) AND ADDRESS(ES) Air Force Research Laboratory/VSBC 29 Randolph Rd Hanscom AFB, MA 01731-3010			8. PERFORMING ORGANIZATION REPORT NUMBER AFRL-VS-TR-1999-1532 E.R.P., No. 1225	
9. SPONSORING/MONITORING AGENCY NAME(S) AND ADDRESS(ES)			10. SPONSORING/MONITORING AGENCY REPORT NUMBER	
11. SUPPLEMENTARY NOTES *Orion Research Co.				
12a. DISTRIBUTION AVAILABILITY STATEMENT Approved for Public Release; Distribution Unlimited			12b. DISTRIBUTION CODE	
13. ABSTRACT (Maximum 200 words) The Mobile Lidar Trailer (MLT) measures backscattering returns from solid rocket booster exhaust plumes in the stratosphere. A worst-case assessment of the stratospheric ozone depletion, often associated with the use of Solid Rocket Motors such as the TITAN IV and the Space Shuttle, is provided. The study is based on the measurement of more than 1500 layers of plume sampled in the altitudes between 15 and 55 km. The results show that less than 2 percent of the ozone column is destroyed in the lidar line-of-sight as a result of the launch. Results are also presented on the fading of the plume return associated with the dispersion of the plume for times between 30 minutes and 3 hours after launch. A comparison with current dispersion models is provided. The measurement and analysis are based on the lidar backscattering signal from the rocket exhaust plume measured at the wavelengths of 308, 355, 532, and 1064 nm for times between 5 and 200 minutes after launch.				
14. SUBJECT TERMS Lidar, Launch vehicle, Exhaust plume, Backscattering, Ozone depletion			15. NUMBER OF PAGES 22	
			16. PRICE CODE	
17. SECURITY CLASSIFICATION OF REPORT UNCLASSIFIED	18. SECURITY CLASSIFICATION OF THIS PAGE UNCLASSIFIED	19. SECURITY CLASSIFICATION OF ABSTRACT UNCLASSIFIED	20. LIMITATION OF ABSTRACT UNL	

## Contents

1. Introduction	1
2. Experimental setup and lidar mode of operation	2
3. Layering of exhaust plume and total ozone loss	4
4. Plume altitudes	6
5. Plume dispersion	7
6. Plume signal vs. altitude	8
7. Discussion and summary	9
References	13

## Illustrations

<b>Figure 1.</b> CCAS Map. MLT is located at Complex 34.	2
<b>Figure 2.</b> Ozone loss in the worst-case scenario.	5
<b>Figure 3.</b> Altitude dependence of thickness.	6
<b>Figure 5.</b> Layer thickness vs. time.	7
<b>Figure 6.</b> Dispersion of the Mie backscattering signal measured at 532 nm.	9
<b>Figure 7.</b> Mie signal as a function of altitude. Mie signal measured at the peak of the plume detected in the 532 nm return is plotted as a function of altitude.	10

## Acknowledgement

The project was funded and sponsored by the Space and Missile Systems Center, SMC/CLN, through the Rocket Impact on Stratospheric Ozone program. Without this support, this series of eleven measurement campaigns to Cape Canaveral Air Station would not have been possible. The assistance of the following Air Force and Aerospace Corporation individuals is duly appreciated: Capt. Brian Laine, Lt. Leonard Garcia, Dr. Martin Ross, Dr. Jerry Gelbwachs, Dr. Paul Mizera, Mr. Doug Schulthess, Mr. Tom Royal, and Mr. Ross Thompson. Team members Robert Farley, Philip Soletsky, Richard Garner, Michael Burka, MSgt. Patrick Connolly, Ronald Frelin, and Gilbert Davidson contributed to the planning, implementation and execution of the campaigns. 45<sup>th</sup> SW and Range Safety squadron personnel maintained safety in the air space above which the lidar operated. The ozone DIAL and multiple wavelength capabilities of the Mobile Lidar Trailer were implemented with valuable support of the Air Force High Frequency Active Auroral Research program office.

# Lidar Measurement of Rocket Exhaust Plume Dispersion and Layering in the Stratosphere

## 1. Introduction

According to Potter<sup>1</sup>, launch vehicles which use solid rocket motors (SRM) such as the Titan IV and space shuttle, emit large quantities of hydrogen chloride, water, and aluminum oxide particles in the atmosphere with smaller amounts of chlorine, carbon monoxide, and carbon dioxide. Approximately two-thirds of the total exhaust is emitted and deposited in the troposphere and the rest in the stratosphere up to 45 km and there have been speculations about the long term and global effects of these launches. In 1998, Jackman<sup>2</sup> suggested that a measurable decrease of the annually averaged global total ozone could be predicted by his model if the alumina emission is dominated by particles of sizes  $\sim 0.012$  micrometers. These submicron particles were measured in Space Shuttle SRM plume by Strand<sup>3</sup>. The speculated effects on stratospheric ozone at the global scale is, however, beyond the scope of this study.

The chemical impact of this emission in the stratosphere also includes the immediate and transient destruction of ozone due to direct discharge of chlorine from the exhaust<sup>4</sup>. As the operating agency of the launch sites where many of these SRM vehicles are launched, the Air Force is concerned about the issues of public health and personnel safety. Modeling studies indicate that this impact is localized near the plume<sup>5</sup>. In-situ measurement of  $\text{Cl}_2$  29 minutes after a twilight Titan IV launch agreed with model predictions that a large fraction of  $\text{HCl}$  is converted to chlorine by afterburning reactions<sup>6</sup>. The measurement results suggest that local and transient ozone decrease could be expected right after daytime launches when  $\text{Cl}_2$  would be photodissociated by solar UV radiation. Nevertheless, except for an earlier report by Pergament<sup>7</sup> for substantial ozone decrease after a daytime Titan III launch, there has been no direct ozone measurement confirming the observation. On the other hand, measurement of the total ozone column with a TOMS (Total Ozone Mapping Spectrometer) device on Nimbus 7<sup>8</sup> showed no measurable loss. Of course, this measurement was conducted near the launch site and the outcome depends strongly on the position of the plume relative to the sensors. Aerospace also reported no substantial decrease of the ozone column using handheld solar UV radiation monitors. Apparently, there exist discrepancies between modeling results, in-situ ozone, and ambient UV measurements. The AFRL MLT lidar was deployed to Cape Canaveral Air Station since 1995 to provide the Air Force Space and Missile Center with experimental data on ozone content in the plume, plume dispersion and particle sizes. The in-plume ozone measurements have failed to yield conclusive results<sup>9</sup>. However, data on the dynamics and dispersion of the plume can be used to elucidate and possibly resolve the mentioned discrepancies.

This report addresses the dynamics and dispersion of plume exhaust for times less than 3 hours after launch. The goal of this report is to establish the direct consequences of plume dynamics to the impact of SRM emission to the local and ambient UV radiation level. In other words, we just focus on the local safety and public health issues. These issues are related to, but not necessarily determined by, the actual ozone reduction predicted by the various models. It is also the goal of this study to document data on the dispersion of exhaust plumes in the stratosphere obtained in the 1995-1998 measurement program sponsored by SMC.

## 2. Experimental setup and lidar mode of operation

Lidar provides a capable tool to measure an SRM exhaust plume that is constantly moved by atmospheric winds. Under normal wind conditions, the plume could be stretched and displaced by as much as 100 km within hours. Attempts to measure the plume with ground-based photography are made difficult because of the unfavorable aspect ratios of the viewing angles. Altitude determination by triangulation is further hindered by a variable wind profile that

### Cape Canaveral Air Force Station

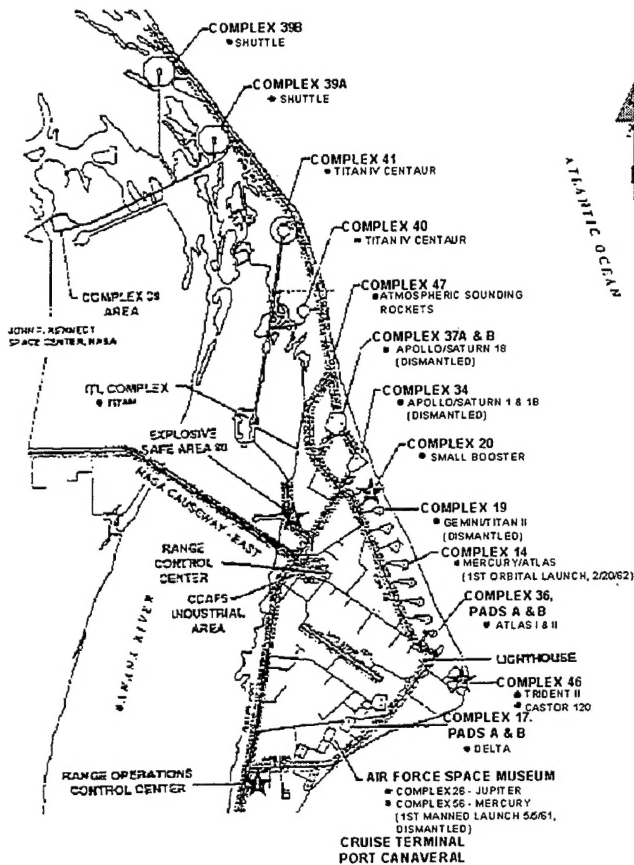


Figure 1. CCAS Map. MLT is located at Complex 34

supported by MLT. The data from the TITAN's and Space Shuttle exhaust plumes are used for this study. Each profile set includes the return at 3 wavelengths. The MLT is centrally located with respect to the various launch pads, and must usually be rotated by crane several days prior to launch in order to optimize the position of the trailer's viewing port. The Titan IVs are launched from Launch Complexes 40 and 41 and the shuttles use Complexes 39A and 39B. Most of the vehicles are launched to the East and to leverage the 55 degree azimuth range of MLT, the laser is typically reoriented prior to launch. The medium-sized vehicles are launched from the Launch Complexes to the south of MLT.

changes direction often in the lower stratosphere hence causing the plume to snake around and often blocking the line of sight. Aircraft have been used to sample the exhaust gas but it is difficult to keep the airplane at stratospheric heights for an extended period. In fact, there are not too many research high-altitude aircraft that can climb to above 19 km. These limitations are compounded by the fact that in the dispersed phase, the plume is often not visible to the pilot. On the other hand, lidar can track the plumes from a distance and observe them for up to 3 hours. The end of an observation session is often determined by safety considerations that keep the laser beam from low elevation angles. Plumes are detected and tracked at altitudes up to 45 km.

Our experiments are conducted from the Mobile Lidar Trailer (MLT), a Rayleigh and differential absorption lidar (DIAL) with the added benefit of a joystick-controlled scanning mirror. The MLT is deployed to Cape Canaveral Air Station (map in Figure 1), Space Launch Complex 34 from where all the data herein were taken over the course of 11 missions and total over 1000 lidar profiles<sup>10</sup>. Table 1 lists the launches



At present, the MLT is capable of operating at four different laser wavelengths, but at only three at one time due to constraints of the optical components employed. A Lambda Physik EMG201 MSC excimer laser with XeCl gas mixture is used to generate 308 nm radiation with a repetition rate of 60 Hz. A Spectra Physics GCR230 Nd:YAG laser provides a 1064 nm fundamental and 532 nm and 355 nm harmonics at a repetition rate of 30 Hz. The system has been run in two basic configurations; one which utilizes the fundamental and both harmonics of the YAG laser, and a second which combines the 355 and 532 nm beams with the 308 nm beam of the excimer. Both cases involve the beams being separated, expanded and recombined for delivery to the atmosphere by a 4-inch kick mirror, which along with the collection mirror, make up the computer-controlled scanner mirror. An autocollimator is used to ensure that the two mirror surfaces are coplanar, thus optimizing detection of the return.

**Table 1. Measurement campaigns.**

Launch Vehicle	Date	Launch Time
Titan IV K-21	Nov 6, 1995	00:15EST
Titan IV K-16	Apr 24, 1996	19:36EST
Titan IVB K-24	Feb 23, 1997	15:20EDT
STS-76	Mar 22, 1996	3:15EST
STS-78	Jun 20, 1996	10:49EDT
STS-79	Sep 16, 1996	4:55EDT
STS-91	Jun 2, 1998	18:06EDT
Atlas-Centaur	Apr 25, 1997	1:49EDT
Delta II	Jul 22, 1997	11:43EDT
Atlas-Centaur	Dec 8, 1997	18:52EST
Atlas II-AS	Mar 16, 1998	20:30EST

The Lidar return is collected by the combination of this 12-inch mirror and a horizontally-positioned telescope. The signal is then chopped (60 Hz shutter), and the various wavelengths are separated and individually detected. Time delays between the flashlamp and Q-switch triggers and between the Q-switch trigger and shutter opening provide a means by which the laser power can be optimized and unwanted low altitude return can be eliminated, respectively. Three Hamamatsu R878 photomultiplier tubes (-1500 V bias) are used to detect the 308, 355 and 532 nm returns, while an Analog Modules silicon avalanche photodiode (RCA C30956E/312-400) is used to monitor the near infrared signal. For collection purposes, the iris is typically set for a field of view of 0.75 mrad.

The signal is buffered by a 47 k $\Omega$  input impedance buffer amplifier (0.7  $\mu$ sec time constant) and fed to our data acquisition computers. Whenever possible, a CAMAC-based photon counting system is used for data acquisition, but proves to be untenable for all but night launches when there is no saturation effects from sunlight. Daytime launches require analog detection techniques. Analog data acquisition for the earlier missions was accomplished by three SONIX64 8-bit digitizer boards that yielded a total of six different analyzer channels. During these missions, CCAS launch control personnel would not allow irradiation of the plume until the launch vehicle was well out of range of our laser beam. This would mean that data collection would not start for at least 30 minutes in most cases, by which time the missile plumes would have dispersed, resulting in reduced return signal. Later missions saw the opening of our data acquisition window reduced to as short as three minutes after launch. In order to assist in locating the plume when the time comes to illuminate, a video camera is mounted to the side of

the collection mirror. The trajectory of the launch vehicle, in addition to rawinsonde data, is obtained prior to launch, and the collection mirror is positioned so that it is pointing at the plume expected location at three minutes after launch. This works exceptionally well for day launches. Illumination of the plume occurs before the exhaust trail is significantly dispersed by stratospheric winds. As a result, it has become necessary to upgrade our system to two 12-bit PDA12 cards (total of four channels) in order to provide the sixteen-fold increase in dynamic range necessary to handle the stronger lidar return signal with the reduced risk of accidental saturation. Generally, the mode of scanning used for the data analyzed here is one in which the lidar is positioned to obtain maximum Mie scattering return at a given altitude. The signal is integrated for an interval suited to the strength of the return and rarely exceeds 900 laser shots, or 30 seconds in the case of the YAG laser. Then, the lidar beam is re-positioned, if necessary, in order to obtain maximum signal. Range resolution of the plume is chosen as 120 meters for the current data acquisition system.

### **3. Layering of exhaust plume and total ozone loss**

In the typical session, the lidar operation is interrupted 5 minutes before launch and permitted to resume at LT+delay. The delay varies and depends on the nature of the launch. With launches of manned spacecraft, the delay is typically 15 minutes. With unmanned spacecraft such as the TITAN IV vehicles, the delay is reduced to about a few minutes. The exact delay is determined by the site personnel on a case by case basis. The initial pointing of the lidar is determined by the forecasted plume position based on the vehicle's trajectory and a measured wind profile. The sampling of the plumes is inevitably biased by the operational preference of altitudes of weak winds and directions afforded by the actual orientation of the MLT.

Figure 2 shows the histogram of observed individual plume thickness. It is observed that the plume is rapidly dispersed into thin layers within 20 minutes from launch time. Rare observations of plume thicker than 1 km are usually witnessed at early times and when the plume layers are aligned on the lidar's line of sight. In general, the histogram shows that almost all layers are less than 250 meters in thickness. The lower plot shows the histogram of total thickness. The total thickness is for all layers observed in a lidar profile. With typical winds of about 5 m/s and plume extension of ~ 1-5 km, the plume resides in the lidar path longer than it takes to make a measurement since the signal integration time is always set at less than 60 seconds. If that is not the case, then the measured total thickness overestimates the instantaneous value. As shown on the right vertical axis, the probability that the observed total thickness is less than the indicated value is also plotted. Note that in 95 percent of the cases, the total thickness is less than 500 meters.

The concern of total ozone loss to the local environment is the main issue addressed by these measurements. If the exhaust plume depletes ambient ozone in the stratosphere, then it is conceivable that the direct path between the sun and a locale is deficient in ozone. This could result in an increase in harmful UV radiation level. The lidar probes the environment in its line of sight or laser path. We assume that the reduction of ozone in the lidar's path is statistically representative of that from the sun. Using the results in Figure 3, one can estimate the gravity of the ozone depletion problem. Figure 3.b shows the histogram of fractional ozone loss as indicated by the plume profiles. To estimate the total ozone column loss, we assume the worst case of total depletion in the exhaust plume. Using the integrated plume thickness as plotted in

Figure 2, the assumption of complete depletion and a typical ozone profile, we compute the integrated ozone loss using the following equation.

$$\frac{\Delta O_3}{O_3} = 1 - \frac{1}{\int n_{O_3}(z_i) \cdot dz} \cdot \sum_i \Delta z_i \cdot n_{O_3}(z_i)$$

Index  $i$  enumerates the number of plume layers present in the line of sight,  $n_{O_3}$  represents ozone density, and  $\Delta z$  plume thickness.

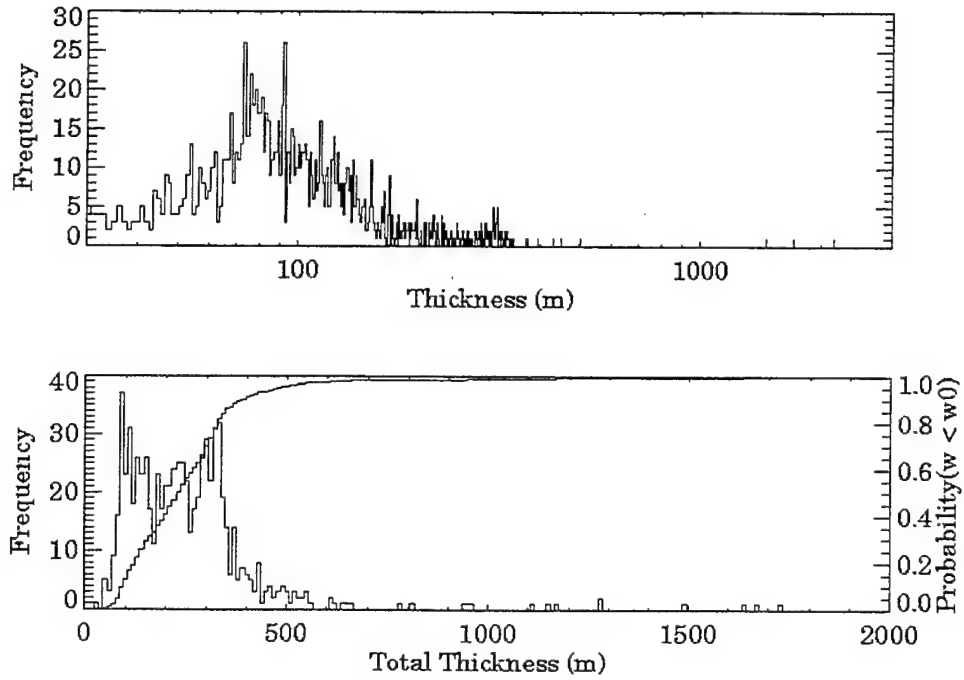


**Figure 2.** Top: histogram of individual plume thickness. Lower: histogram of total plume thickness. The probability of observing a total thickness greater than the indicated value is also plotted (using the right vertical axis).

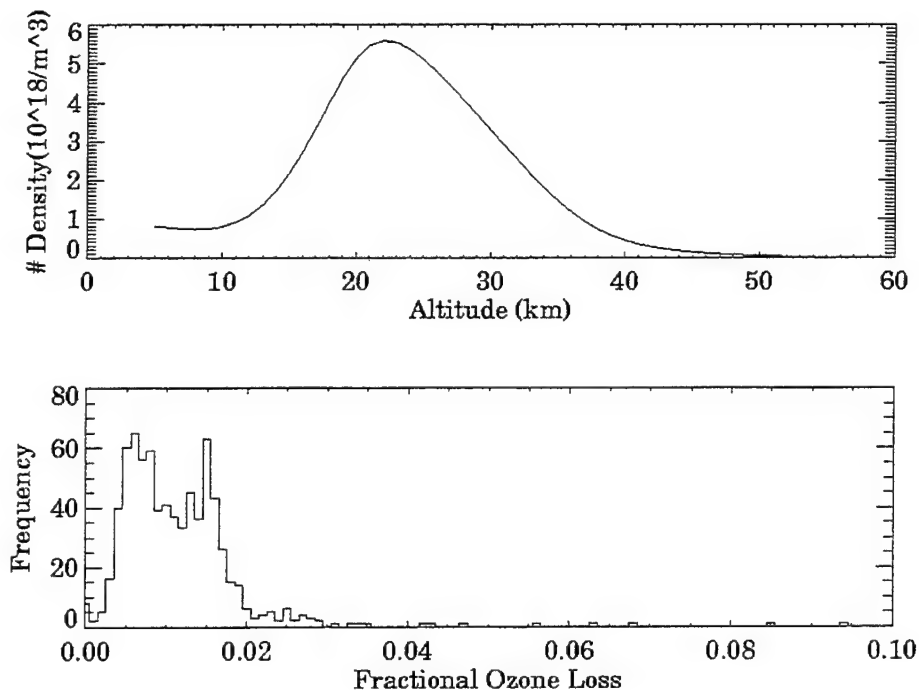


**Figure 3.** Ozone loss in the worst-case scenario. Top: Model ozone profile. Bottom: Histogram of total ozone column depletion.

In Figure 3, it is evident that the column loss of ozone is never more than 2 percent in more than 95 percent of the observations. While this sampling might not provide an exact approximation of the ozone loss in the sun direct path, the magnitude of this problem is minimal. The dispersion of the plume has rapidly negated the UV radiation problem in areas near the launch site or under the plume.

#### 4. Plume altitudes

As it turned out, plumes are mostly observed in the stratospheric heights which coincide with the ozone layer. Figure 4 shows the histogram of plume altitudes. The average wind profile for Cape Canaveral is also overlaid for comparison. It is worth noting that the heights at which plumes are most likely to be probed correspond with the region of weakest winds. In the region above 25 km where wind velocity becomes appreciable, the zonal component has a predictable seasonal dependence. This predictability is used to align MLT in an orientation that keeps the plume accessible to the lidar for a long while after launch. The layer's thickness does not show a systematic dependence on height, as indicated in Figure 4. The average wind profile measured at the Kennedy Space Center<sup>11</sup> is also plotted to show that plumes are most frequently observed in the the region of lowest wind speeds. It is worth noting that plumes are detected at altitudes up to 55 km. Figure 5 shows the lack of any obvious trend of the measured thickness. This constancy of the layer thickness can be attributed to (a) a slow vertical diffusion and/or (b) the effect of wind shear.

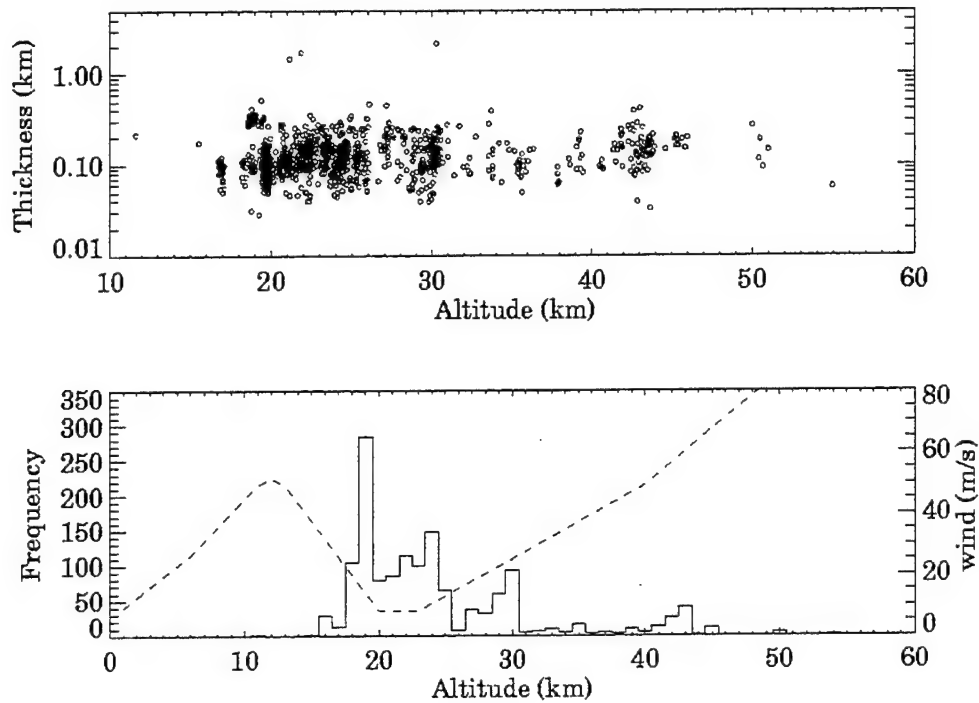


**Figure 4.** Altitude dependence of thickness.

- a) Scatter plot of measured plume thickness as a function of altitude.
- b) Histogram plot of observed plumes in altitude bins. The overlaid plot (dashed) represents the average wind magnitude for Cape Canaveral according to NASA/CR-1998-208859.

## 5. Plume dispersion

The localized problem of ozone depletion as modeled in previous modeling efforts (Brady and Martin<sup>5</sup>) such as, because of their inherent chemical reactions, depend critically on the dimension and the dispersion of the plume. Experimental data on plume dispersion are far from being complete. While direct lidar results on the plume dimension have been presented elsewhere<sup>12</sup>, in this report we will compare the lidar signal fading with predictions by current dispersion models. The MLT lidar backscattering signal has been observed for up to 3 hours after launch. With the assumption that the backscattering coefficient is proportional to particle density, the fading of plume signal describes its dispersion. In the first 20-30 minutes following the launch, there have been speculations that the composition of the plume particles is still evolving in the stratosphere (Dentamaro paper). The change is derived from the observation that the ratio of backscattering signals measured at two different wavelengths is changing during the

initial phase and asymptotically approaching a constant level. The assumption that the composition remains fixed in the later phase, as indicated by a stable final ratio, can be justified for times later than T+30 min.

Using data from Space Shuttle reported by Watson et al.<sup>13</sup>, Brady et al.<sup>5</sup> derived a formula for the chemical concentration in the plume such that

$$n(t) = \frac{n_0}{1 + \left[ (2 \cdot 10^{-3} \cdot s^{-1}) \cdot t \right]^{2.6}}$$

where t is expressed in seconds. For t greater than 20 minutes, the time dependence is roughly t to the power of -2.6. On the other hand, Denison's model<sup>14</sup>, based on a scale dependent diffusivity, can be expressed as

$$n(r,t) = n_0 \left( \frac{t_0}{t} \right)^2 \exp \left[ -\frac{1}{b} \cdot \left( \frac{r}{t} - \frac{r_0}{t_0} \right) \right]$$

It predicts a time dependence of t to the power of -2 measured at the peak of the plume or zero radial distance r. Both expressions are plotted in Figure 6 as the dashed (Brady and Martin) and dash-dotted (Denison) lines. Backscattering coefficients are determined from the normalized Mie return and by tying it to the USSA 1976 model atmospheric density at 16 km. When compared to the scatter plot of the backscattering coefficients, it should be noted that the model time dependence lines are for the peak of the plume layer, and should be considered as the upper envelopes of the backscattering points which sample the plume at any possible radial distance. While both models agree with the data, a slightly better agreement to Denison's is suggested by the plot. In Figure 6, the solid line represents the density of particles using a top-hat distribution and the measured plume dimensions reported by Dao<sup>12</sup>. The dimensions are listed here for reference.

**Table 2. Plume expansion.**

Time (hr)	0.8	1.2	1.6
Plume dimension (km)	3.	6.5	11

The lack of agreement between the solid line which is plotted to be inversely proportional to d<sup>2</sup> suggests that the top-hat distribution is not a valid assumption in representing the dispersion signal correctly.

## 6. Plume signal vs. altitude

Lidar backscattering is used to provide a self-calibrated measurement of the plume backscattering coefficient. In a lidar profile, the return from the plume is superimposed on the return from clear air. Backscattering return from the clear atmosphere is due to Rayleigh scattering from molecules. Therefore, the Rayleigh signal is directly related to atmospheric density. By normalizing the plume signal to the Rayleigh signal at a calibration point, one can relate the Mie signal to atmospheric density using the known Rayleigh cross section. Since a model (e.g., USSA 1976) can be used to estimate the density at the tie point, this relationship is used to infer the Mie backscattering coefficient. In most cases, we chose the tie point below the

lowest plume and above a height of 14 km where cirrus clouds could be found. The uncertainty of the density calibration is better than 5% and the absolute measurement of plume Mie scattering is typically limited by the return signal to noise ratio. At the plume altitude, the Rayleigh component is subtracted from the total signal to obtain the Mie component. In Figure 7, the Mie return from the plume peak is plotted against altitude. On the same plot, the HCl emission profile is also shown. If the amount of emitted HCl is representative of the total exhaust, then the Mie profile seems to agree with and follow the emission profile.

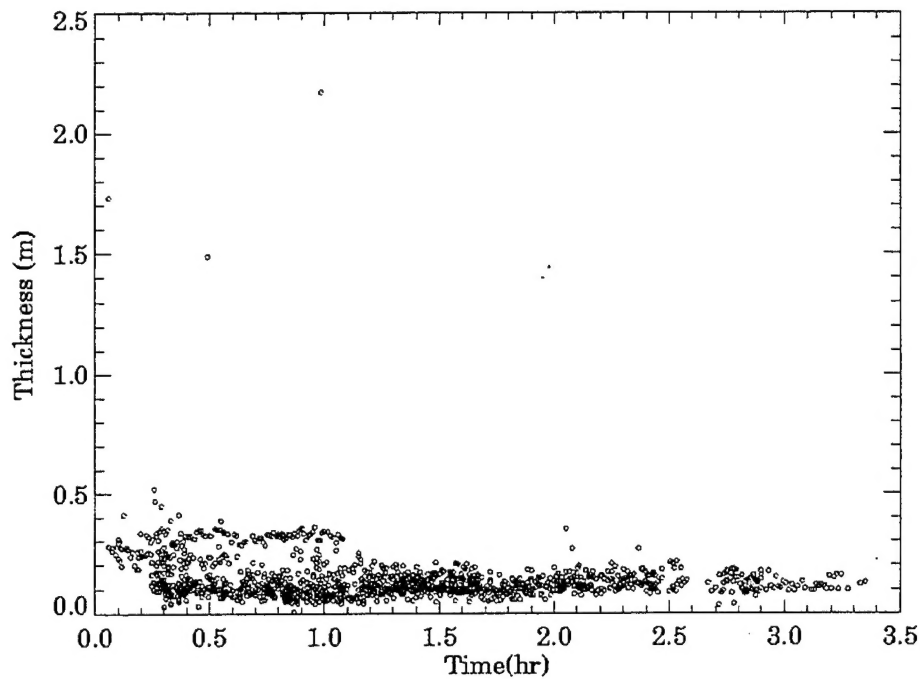


**Figure 5.** Layer thickness vs. time

## 7. Discussion and summary

The results have shown that launch vehicle exhaust plume rapidly disperses into thin layers, almost always less than 250 meters. The total plume column height in a typical line of sight is less than 500 m. These observations have a direct impact on the RISO research objective. Assuming that ozone is completely depleted in the plume, the “worst-case” ozone column loss is still less than 2 percent in a representative line of sight. The results point to a minimal impact of the exhaust plume to the local UV radiation level. The layering is observed to take place as early as 10 minutes after launch. This layering mechanism is observed in summer as well as in winter wind conditions. The altitudes sampled by these measurements range from 15 to 55 km. The altitudes of most frequent observations correspond with the region between the tropopause and the stratopause.

The dispersion of the plume also results in the decay of the plume number density at the center of the plume. This dispersion is observed via the evolution of the plume return. The decay of the backscattering suggests a time dependence of  $t$  to the power of  $-2.0$  to  $-2.6$ , in agreement with current dispersion models. Lidar techniques are shown to be a convenient diagnostic tool to observe and study an exhaust plume over a period of hours after the launch.

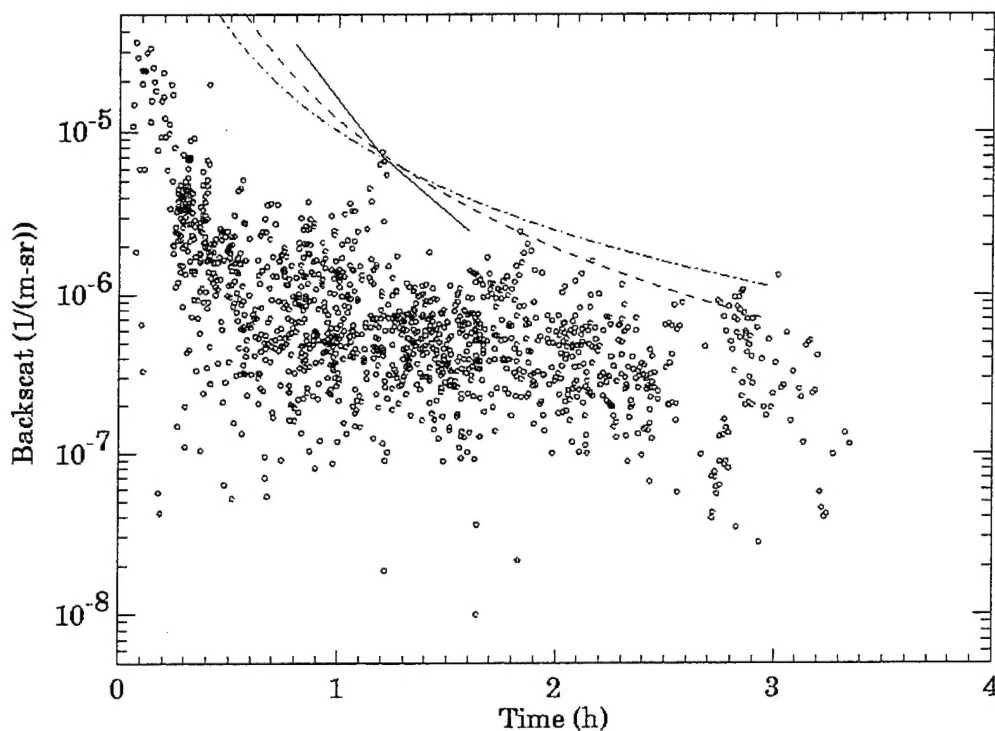


**Figure 6.** Dispersion of the Mie backscattering signal measured at 532 nm. The Mie signal measured at the peak of the plume return is plotted against time of observation relative to launch time. Solid is derived from plume dimension. The dash and dash-dot lines show dispersion models.



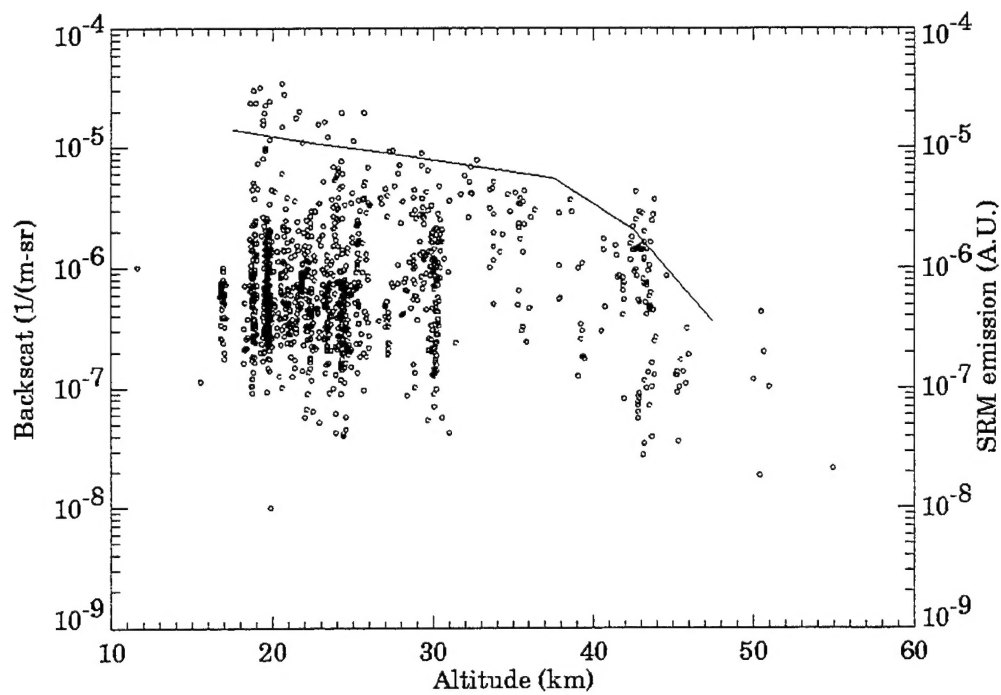


**Figure 7.** Mie signal as a function of altitude. Mie signal measured at the peak of the plume detected in the 532 nm return is plotted as a function altitude. The solid line depicts the exhaust emission altitude profile as represented by the amount of HCl gas emission (Prather, 1990).

## References

---

- <sup>1</sup> Potter A. E., Environmental Effects of the Space Shuttle, *J. Environ. Sci.* 21, 15-21, 1978.
- <sup>2</sup> Jackman, C.H., Cosidine, D.B. and Fleming, E.L., A global modeling study of solid rocket aluminum oxide emission effects on stratospheric ozone, *Geophys. Res. Lett.* 25, 6, 1998.
- <sup>3</sup> Strand, L.D., Bowyer, J.M., Varsi, G., Laue, E.G. and Gauldin, R., Characterization of particulates in the exhaust plume of large solid propellant rockets, *J. Spacecraft and Rockets*, 18, 1981.
- <sup>4</sup> Prather, M.J., Garcia, M.M., Douglas, A.R., Jackman, C.H., Ko, M.K.W., and Sze, N.D., The space shuttle's impact on the stratosphere, *J. Geophys. Res.*, 95, 1990.
- <sup>5</sup> Brady, B.B. and Martin, L.R., Modeling solid rocket booster exhaust plumes in the stratosphere with SURFACE CHEMKIN, The Aerospace Corporation, El Segundo, CA, TR-95(5231)-9 or SMC-TR-96-19
- <sup>6</sup> Ross, M.N., Ballenthin, J.O., Gosselin, R., Meads, R.W., Zittel P.F., Benbrook, and J.B., Sheldon, In-situ measurement of Cl<sub>2</sub> and O<sub>3</sub> in a stratospheric solid rocket motor exhaust plume, *Geophys. Res. Lett.*, 24, 1997.
- <sup>7</sup> Pergament, H.S., Gomberg, R.I., and Polpoff, I.G., Proceedings of the Space Shuttle Environment Assessment Workshop on Stratospheric Effects, NASA Tech. Memo X-58198, 1977.
- <sup>8</sup> McPeters, R., Prather, M.J., and Jackman, C.H., Reply to Aftergood (1991), *J. Geophys. Res.*, 96, 1991.
- <sup>9</sup> Lidar results on STS-76 by our group showed no change in the ozone level with error bar equal to 10 percent of the ambient level.
- <sup>10</sup> Dentamaro, A.V., Dao, P.D., Farley, R., and Ross, M., Characterization of Particles from Stratospheric Launch Vehicle Plumes using Wavelength-dependent Lidar Techniques, *Geophys. Res. Lett.*, vol. 26, No. 15, 2395 (1999).
- <sup>11</sup> Smith, O. E. and Adelfang, S. I., A Compendium of Wind Statistics and Models for the NASA Space Shuttle and Other Aerospace Vehicle Programs, NASA/CR-1998-208859 (Oct. 1998.)
- <sup>12</sup> Dao, P.D., Gelbwachs, J.A., Farley, R., Garner, R., Soletsky, P., and Davidson, G., LIDAR stratospheric SRM exhaust plume measurements, AIAA 35<sup>th</sup> Aerospace Sciences Meeting, 97-0526, 1997.
- <sup>13</sup> Watson, R.T., Smokler, P.E., and Demore, W.B., An assessment of F<sub>2</sub> and N<sub>2</sub>O<sub>4</sub> atmospheric injection from an aborted space shuttle mission, NASA JPL Publication 77-81, 1978.
- <sup>14</sup> Denison, M.R., Lamb, J.J., and Bjorndahl, W.D., Wong, E.Y. and Lohn, P.D., Solid rocket exhaust in the stratosphere: Plume diffusion and chemical reactions, AIAA 92-3399, 1992.